Mammalian Biology
https://doi.org/10.1007/s42991-023-00388-x

SHORT COMMUNICATION

Foramen ovale as a new determinative sign for the identification of tiger (*Panthera tigris*) and lion (*Panthera leo*) skulls

Dominika Formanova[1] · Martin Pyszko[2] · Ondrej Horak[2,3] · Jolana Sadkova[1] · Pavla Rihova[1] · Anna Kubatova[1]

Received: 11 April 2023 / Accepted: 1 December 2023
© The Author(s) 2024

Abstract
Tiger and lion bones are valued highly on the wildlife black market. The skeletons of the two species are very similar, but the level of protection and the laws applicable to them differ. When detecting crime in the field, it can be crucial to recognize the skeletons of these two species by their morphological features. A distinguishing feature neglected in practice is the *foramen ovale* at the base of the skull. A total of 112 skulls were evaluated (55 tigers and 57 lions). The orientation and appearance of the *foramina ovalia* were analyzed on skull photographs. Significant differences were found between tigers and lions. In lions, the *foramina ovalia* faced laterally and their outlets were usually at least partially hidden behind the straight edge of the *os basisphenoidale* from the ventral view of the skull. In most adult tigers, the *foramina ovalia* faced more rostrally with their outlets visible and bounded by a semi-circular edge of the *os basisphenoidale*. However, tiger skulls exhibited higher variability in *foramina ovalia* orientation than lion skulls. Like other identifying features on tiger and lion skulls, the *foramen ovale* was unable to distinguish all skulls with 100% confidence. Nevertheless, knowledge of this structure can help considerably in species identification.

Keywords Craniometry · Morphology · Pantherinae · Skull differences · Skull identification · Wildlife crime

Tiger (*Panthera tigris*) skeletons, as well as individual bones, skulls, teeth, and claws, are very lucrative commodities on the wildlife black market (Mills and Jackson 1994; Wong and Krishnasamy 2022; Nittu et al. 2023). Demand in Asian countries far outstrips illegal supply, so tiger bones are often counterfeited and interchanged for lion (*Panthera leo*) bones due to their strong similarity (Williams et al. 2015a, b; EIA 2017; Williams et al. 2017). The ability to distinguish tiger and lion skeletons based on morphological features can be very useful when working with law enforcement in the field. Several deterministic characters of tiger and lion skulls are described in the literature (Blanford 1888; Boule 1906; Pocock 1929; Merriam and Stock 1932; Haltenorth 1936, 1937; Hemmer 1966; Christiansen 2008; Christiansen and Harris 2009). Unfortunately, none of these hallmarks is 100% reliable, and a combination of several is necessary to minimize the possibility of confusion (Christiansen 2008). For fieldwork, it is preferable to use easily recognizable hallmarks that can be inspected even from photographs of the skull, and which can be consulted with a zoological expert remotely. One of the so far neglected determinative structures is the *foramen ovale* and its orientation on the cranial base. The *foramen ovale* is an opening in the wing of the *os basisphenoidale*. In cats, it is found in the space between *foramen rotundum* and *fissura sphenopetrosa*. Laterally from the *foramen ovale*, erected joint surfaces of the jaw joint are bordered from the rear by protrusions *processus retroarticulares*. Caudally, the *foramen ovale* is adjacent to the *processus muscularis* protruding from the *bulla tympanica* of the temporal bone. Differences in the *foramen ovale* in tigers and lions are mentioned by Haltenorth (1936, 1937) or Hemmer (1966), but the potential of this hallmark to distinguish between species has not been formally assessed.

Handling editor: Gabriele Sansalone.

✉ Dominika Formanova
dominika.formanova@natur.cuni.cz

[1] Institute for Environmental Studies, Faculty of Science, Charles University, Prague, Czech Republic

[2] Department of Anatomy, Histology and Embryology, University of Veterinary Sciences Brno, Brno, Czech Republic

[3] Department of Pathology and Parasitology, State Veterinary Institute Prague, Prague, Czech Republic

Published online: 05 January 2024

The material for this study consisted of 112 dried skulls of big cats (Table 1). Skulls with fully developed permanent dentition were classified as adults, and skulls with fully or partially deciduous dentition as juveniles. Both adults and juveniles were included in the study so that the new determinant feature could be assessed in as wide a range of individuals as possible. Studies dealing with the morphology of tiger and lion skulls often work with skulls of adult animals only (Christiansen 2008). However, to combat illegal trade, it is necessary to identify juvenile skulls as well as adult skulls. Therefore, records of the morphological structure of juvenile skulls were considered as also important.

The subspecies by Wilson and Reeder (2005) have been recorded in 36 tiger skulls (19 *P.t.altaica*, 4 *P.t.corbetti*, 1 *P.t.sondaica*, 11 *P.t.sumatrae*, and 1 *P.t.tigris*) and in 20 lion skulls (2 *P.l.bleyenberghi*, 5 *P.l.leo*, and 13 *P.l.persica*). The skulls came from several sources: Czech National Museum, zoological gardens of the Czech Republic and Slovakia, University of Veterinary Sciences Brno, Faculty of Science of Charles University in Prague, Czech Environmental Inspectorate, and Customs Administration of the Czech Republic. Six tiger and 6 lion skulls originated from animals in the wild, 42 tiger and 36 lion skulls were from animals bred in captivity, and the origin of 7 tiger and 15 lion skulls was unknown. Whilst interpopulation variation and captivity status are known to influence skull morphology in both species (Zuccarelli 2004; Mazák 2010a, b; Yamaguchi et al. 2013; Hartstone-Rose et al. 2014; Cooper et al. 2022), these factors were not included in the analysis due to limited sample size. The morphology of the skull can also be influenced by the health status of the animal (Shamir et al. 2008; Saragusty et al. 2014), therefore, only skulls without obvious deformities were used in this study.

Two parameters were measured from the skulls using a vernier calliper (Fig. 1):

(1) Greatest skull length (GSL): the length from the most anterior part of the rostrum (excluding teeth) to the most posterior point of the skull.
(2) Zygomatic breadth (ZB): the greatest distance between the outer margins of the zygomatic arches.

Digital photographs in high resolution (6000 × 4000 pixels) were taken of each specimen using a NIKON D5500 digital camera. To evaluate the orientation and appearance of the *foramina ovalia*, an image of the ventral aspects of each skull was used. For each photograph, the appearance of the prominence of the left (LFO) and right (RFO) *foramen ovale* was described. The orifice of the *foramen ovale* could be bordered by a semi-circular margin of the *os*

Table 1 Species, sex, and age of the tested individuals

	Tiger ($n=55$)		Lion ($n=57$)	
	Adult ($n=49$)	Juvenile ($n=6$)	Adult ($n=45$)	Juvenile ($n=12$)
Male	14	2	14	4
Female	24	0	18	6
Unknown sex	11	4	13	2

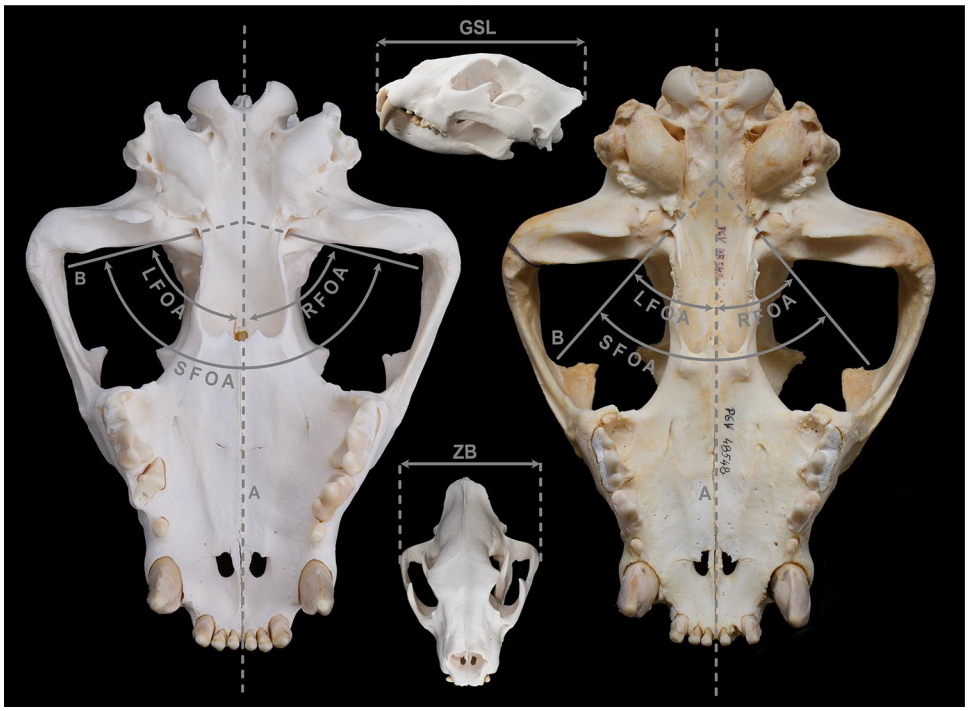

Fig. 1 Lion and tiger skulls from ventral view, visualization of the parameters measured: GSL—greatest skull length, ZB—zygomatic breadth, A—the midline, boundary between the left and right half of the skull, B—the direction of the line passing through the *foramen ovale*, LFOA—the angle of the left *foramen ovale* (angle between A and B on the left), RFOA—the angle of the right *foramen ovale* (angle between A and B on the right), SFOA—the angle that the two *foramina ovalia* make together (LFOA + RFOA). Origin of the skulls presented: left and middle—lion skull *Panthera leo bleyenberghi*, adult female, collection of the Lesna Zoo, ID Lesna2; right—tiger skull *Panthera tigris altaica*, adult female, collection of the Czech Nat. Museum, ID 48548

basisphenoidale (C) and thus completely visible (V), or it could be obscured behind the straight margin of the *os basisphenoidale* (S) and either completely hidden (H) or partially visible (V). The orientation of the LFO and RFO in all photographs was examined independently by two observers (O1 and O2), each of them taking two measurements (trials a and b) at least 1 week apart. They established the midline "A" (the exact boundary between the left and right halves of the skull) and a line passing in the direction of the *foramen ovale* projection "B". The angle between these two lines was measured on both sides of the skull using MB-Ruler 5.4 software (Markus Bader, MB-Softwaresolutions, 2022) and expressed as an integer. Thus, for each skull, four sets (O1a, O1b, O2a, O2b) of the following data were obtained: the angle of the left *foramen ovale* (LFOA), the angle of the right *foramen ovale* (RFOA), and the angle that the two *foramina ovalia* make together (SFOA) (Figs. 1, 2, for data see SI1).

The intra- and inter-observer reliability of measured values of LFOA and RFOA were tested in SPSS 28.0.1.0 (IBM SPSS Inc., 2021) using the intraclass correlation coefficient (ICC) and standard error of measurement (SEM) (Weir 2005). Reliability analysis with a two-way mixed model was applied (Koo and Li 2016) to all skull samples except the skull with ID Sumi ($n = 111$). This skull was not evaluated by one of the observers due to the quality of the photograph (perceived as of too low quality for evaluation by O2). The results of intra- and inter-observer reliability are presented in Table 2.

According to Koo and Li (2016), ICCs of O1 and O2 indicate good (0.75–0.90) and excellent (greater than 0.90) intra observer reliability, respectively. The inter-observer reliability varied from moderate (0.50–0.75) in RFOA measurements to good (0.75–0.90) in LFOA measurements. Based on the results, the following analyses were counted separately for all datasets (O1a, O1b, O2a, O2b) to be sure of the reliability of the conclusions. Further results are valid for all four datasets.

Tests of normality, assumptions for linear discriminant analysis (LDA), and decision trees were calculated in SPSS 28.0.1.0 (IBM SPSS Inc., 2021). Further analyses were processed in TIBCO Statistica 14.0.0.15 (TIBCO Software Inc., 2021) and included data from all 112 skulls unless stated otherwise. Based on the results of Shapiro–Wilk, and Kolmogorov–Smirnov tests (Table 3), nonparametric measures and tests were used beside the chi-squared test. Specifically, Spearman correlation coefficients (ϱ), Kendall rank

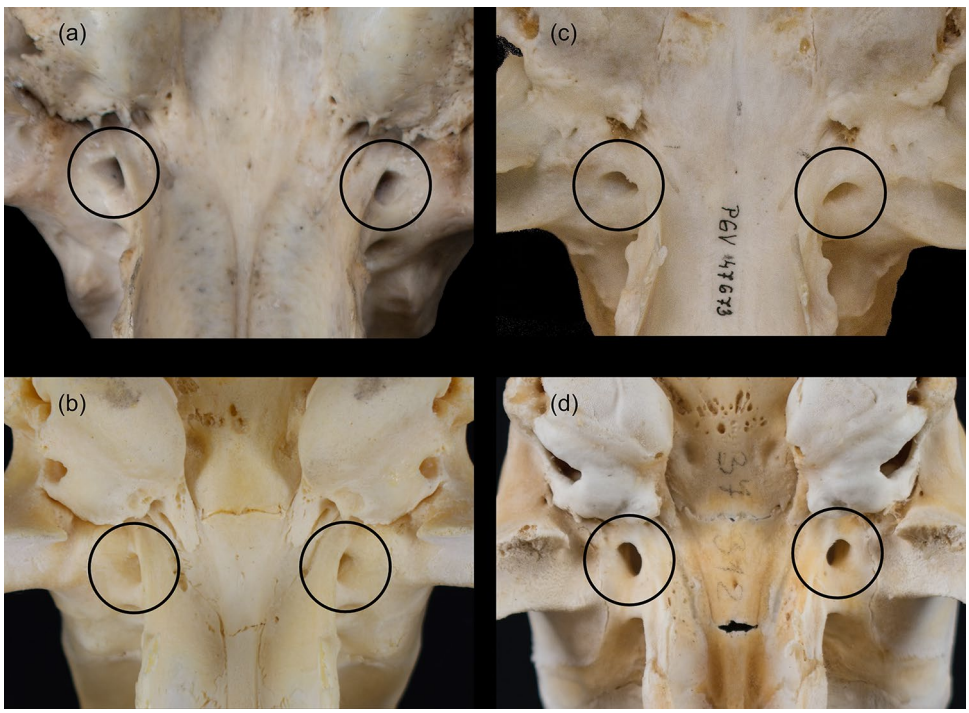

Fig. 2 *Foramina ovalia* (highlighted with circles), detailed view of lion and tiger skulls from the ventral side: **a** adult lion skull, *foramina ovalia* directed laterally with their outlets partially hidden behind the straight edge of the *os basisphenoidale* (*Panthera leo*, adult female, collection of the Czech National Museum, ID 12082); **b** juvenile lion skull, *foramina ovalia* directed laterally with outlets entirely hidden (*Panthera leo persica*, juvenile female, collection of the Czech National Museum, ID 46396); **c** adult tiger skull, *foramina ovalia* facing in rostral direction with their outlets bounded by a semi-circular edge of the *os basisphenoidale* (*Panthera tigris corbetti*, adult female, collection of the Czech National Museum, ID 47673); **d** juvenile tiger skull, *foramina ovalia* directed laterally with outlets entirely visible (*Panthera tigris altaica*, juvenile, sex unknown, collection of the Ostrava Zoo, ID 37312)

Table 2 The results of intra (absolute agreement type analysis, results concerning single measures) and inter (consistency type analysis, results concerning single measures) observer reliability

Reliability		ICC	95% CI	SEM	*P*
Intra	O1-LFOA$_{a/b}$	0.884	0.824–0.923	11.209°	< 0.001
	O1-RFOA$_{a/b}$	0.884	0.807–0.927	11.209°	< 0.001
	O2-LFOA$_{a/b}$	0.993	0.989–0.995	4.143°	< 0.001
	O2-RFOA$_{a/b}$	0.993	0.990–0.995	4.143°	< 0.001
Inter	LFOA$_a$	0.784	0.701–0.847	18.988°	< 0.001
	LFOA$_b$	0.769	0.680–0.835	18.822°	< 0.001
	RFOA$_a$	0.709	0.603–0.791	20.782°	< 0.001
	RFOA$_b$	0.690	0.579–0.776	20.415°	< 0.001

ICC and SEM refers to intraclass correlation coefficient and its standard error of the measurement, respectively. CI refers to confidence intervals

correlation coefficients (τ), and Mann–Whitney *U* tests were calculated. The datasets did not meet the assumptions for LDA calculation differentiating the species based on SFOA, GSL, and ZB (Box's Test of Equality of Covariance Matrices: $P_{O1a} < 0.001$, $P_{O1b} < 0.001$, $P_{O2a} < 0.001$, $P_{O2b} < 0.001$). Instead, decision trees were calculated as an alternative (Feldesman 2002) with one ($x = 1$) as a minimal number of cases in both parent and child nodes. A significance level $\alpha = 0.05$ was established for all calculations. All results were rounded to three decimal places except the values in %, which were rounded to one decimal place.

Lion skulls typically showed *foramina ovalia* directed laterally (Fig. 2a—adult, Fig. 2b—juvenile). From the ventral view, 89.5% ($n = 51$) of lion skulls, including all juveniles, showed at least one outlet of *foramen ovale* fully or partially hidden behind the straight edge of the *os basisphenoidale*. Both outlets of *foramina ovalia* were entirely hidden from ventral view in 49.1% of cases ($n = 28$).

As expected, adult individuals reached significantly higher values of GSL ($U = 17.000$, $Z = 4.942$, $P < 0.001$) and ZB ($U = 6.000$, $Z = 5.142$, $P < 0.001$) than juveniles. On the other hand, no significant difference was found between the *foramen ovale* angles of adults and juveniles, regardless of whether the LFOAs, RFOAs, or SFOAs were compared except for significantly higher SFOAs of juvenile individuals in the dataset O1b, SI2a. Due to the exception in the dataset O1b, only the skulls of adult individuals were included in further analyses. Skulls of adult males showed significantly higher values of GSL ($U = 35.000$, $Z = -3.438$, $P < 0.001$) and ZB ($U = 27.500$, $Z = -3.723$, $P < 0.001$) when compared to adult females. However, no significant difference was found between the *foramen ovale* angles of adult males and females, regardless of whether the LFOAs, RFOAs, or SFOAs were compared ($P > 0.05$ in all cases), SI2a.

No significant correlation was found between any of the *foramen ovale* angles and GSL or ZB except for a weak negative correlation (Schober et al. 2018) between GSLs and RFOAs in the O1a dataset ($\varrho = -0.311$, $P = 0.038$ and $\tau = -0.216$, $P = 0.037$; $P > 0.05$ in all other cases), SI2b.

In adult tiger skulls, the *foramina ovalia* were oriented more rostrally (Fig. 2c), however, values of LFOA and RFOA were much more variable than in lions (Fig. 3). The outlets of the *foramina ovalia* were in 65.3% of cases bounded by a semi-circular edge of the *os basisphenoidale* and therefore visible ($n = 32$), in 14.3% of cases, there were straight edges obscuring the *foramina ovalia* ($n = 7$), and in 20.4% of cases, there was a combination of one *foramen ovale* bounded by the semi-circular edge and the second one bounded by a straight edge ($n = 10$). In 88.2% of cases, when there was at least one straight edge of the *os basisphenoidale*, the outlets of both *foramina ovalia* were still visible ($n = 15$). In juvenile tigers (Fig. 2d), the *foramina ovalia* were directed more laterally, wide open, and entirely visible.

Table 3 Results of normality tests in selected variables (significant results are marked by an asterisk)

Variable	Species	Kolmogorov–Smirnov			Shapiro–Wilk		
		Z	df	*P*	*W*	df	*P*
GSL	*P. leo*	0.110	56	0.086	0.925	56	0.002*
	P. tigris	0.179	54	< 0.001*	0.852	54	< 0.001*
ZB	*P. leo*	0.113	56	0.071	0.936	56	0.005*
	P. tigris	0.186	54	< 0.001*	0.886	54	< 0.001*
SFOA O1a	*P. leo*	0.130	56	0.019*	0.959	56	0.052
	P. tigris	0.082	54	0.200	0.983	54	0.641
SFOA O1b	*P. leo*	0.143	56	0.006*	0.912	56	< 0.001*
	P. tigris	0.071	54	0.200	0.980	54	0.507
SFOA O2a	*P. leo*	0.245	56	< 0.001*	0.734	56	< 0.001*
	P. tigris	0.236	54	< 0.001*	0.705	54	< 0.001*
SFOA O2b	*P. leo*	0.234	56	< 0.001*	0.749	56	< 0.001*
	P. tigris	0.234	54	< 0.001*	0.667	54	< 0.001*

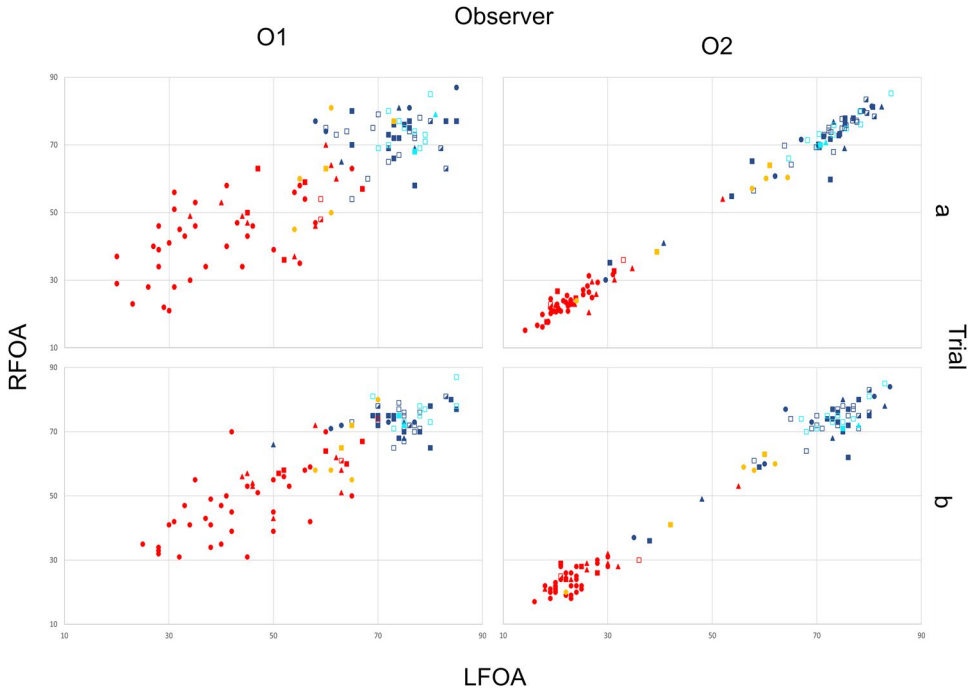

Fig. 3 *Foramina ovalia* angles and shapes in all studied skulls: LFOA—the angle of the left *foramen ovale*, RFOA—the angle of the right *foramen ovale*, O1—observer 1, O2—observer 2, red—*Panthera tigris* adult, orange—*Panthera tigris* juvenile, dark blue—*Panthera leo* adult, light blue—*Panthera leo* juvenile, ■—straight edges of the *os basisphenoidale*, ●—semi-circular edges of the *os basisphenoidale*, ▲—one *foramen ovale* with the straight edge and second *foramen ovale* with the semi-circular edge of the *os basisphenoidale*, fully colored—*foramina ovalia* visible, uncolored—*foramina ovalia* hidden, half colored—one *foramen ovale* visible and second *foramen ovale* hidden

As in lions, adult tigers reached significantly higher values of GSL ($U=0.000$, $Z=3.955$, $P<0.001$) and ZB ($U=0.000$, $Z=3.955$, $P<0.001$) than juveniles. Juvenile tigers showed significantly higher values of the *foramina ovalia* angles than adults [$P<0.01$ in all cases, (Fig. 3, SI2c)]. Therefore, only the skulls of adult individuals were included in further analyses. In adult skulls, both GSL ($U=74.000$, $Z=-2.829$, $P=0.005$) and ZB ($U=90.000$, $Z=-2.345$, $P=0.019$) were found to be significantly higher in males than in females, but no significant difference was found between the *foramen ovale* angles of adult males and females, regardless of whether the LFOAs, RFOAs or SFOAs were compared except the dataset O1b where the males showed significantly bigger angles than females, SI2c.

No correlation was found between any of the *foramen ovale* angles and GSL or ZB in adult tigers ($P>0.05$ in all cases), SI2d.

GSL did not significantly differ between species (all skulls: $U=1454.000$, $Z=0.658$, $P=0.511$; adult skulls only: $U=882.500$, $Z=1.661$, $P=0.097$). However, lions showed significantly higher values of ZB in comparison with tigers when the skulls of adult individuals were considered ($U=816.500$, $Z=2.008$, $P=0.045$). Measurements of the observed angles in photographs revealed a significant difference between the angles (LFOA, RFOA, and SFOA) at which the *foramina ovalia* emerged in lions and tigers (Table 4).

The results showed a significant relationship between the species and the shape of the bordering of *foramina ovalia* (LFO: $\chi^2=47.105$, df = 1, $P<0.001$; RFO: $\chi^2=34.350$, df = 1, $P<0.001$). Similarly, the relationship between species and visibility of the *foramen ovale* was significant (LFO: $\chi^2=34.688$, df = 1, $P<0.001$; RFO: $\chi^2=32.643$, df = 1, $P<0.001$). The shapes of the bordering of *foramina ovalia* and their visibility in connection to the species and age of tested individuals are available in Table 5.

No relationship between the visibility of *foramen ovale* and sex of a lion was found (LFO: $\chi^2=0.127$, df = 1, $P=0.721$.; RFO: $\chi^2=0.072$, df = 1, $P=0.789$). However, a significant relationship was found between the visibility of *foramen ovale* and age of a lion (LFO: $\chi^2=5.134$, df = 1, $P=0.023$.; RFO: $\chi^2=7.118$, df = 1, $P=0.008$). The visualization of the differences in *foramina ovalia* appearance including angles in all studied skulls is shown in Fig. 3.

Selected variables (SFOA, GSL, ZB, LFO/RFO edge and visibility) were input as independent variables in the decision trees calculated from the data of all studied individuals except one lion and one tiger skull ($n=110$). The overall predictability of the species ranged from 81.1 to 97.3%. The first classification step was always based on the assessment of SFOA which was always accompanied by either ZB (O1a and O2b) or GSL (O1b and O2a). LFO/RFO edge did not appear in the decision tree of any dataset. The visibility of LFO/RFO appeared as a variable improving the accuracy only in the dataset O1a. For details see SI3.

The studied characteristics of *foramen ovale* appear to be useful hallmarks to help distinguish between the skulls of lions and tigers. All sets of observations reached significant differences between lions and tigers, although one of the observers reached only good level of intra-observer

Table 4 Results of comparing LFOA, RFOA, and SFOA between lions and tigers by the Mann–Whitney *U* test (significant results are marked by an asterisk)

FOA	Trial	All skulls			Adult skulls only		
		U	*Z*	*P*	*U*	*Z*	*P*
LFOA	O1a	74.000	8.689	< 0.001*	40.000	8.038	< 0.001*
	O1b	64.000	8.748	< 0.001*	41.000	8.030	< 0.001*
	O2a	39.500	8.844	< 0.001*	13.000	8.199	< 0.001*
	O2b	25.500	8.927	< 0.001*	4.000	8.268	< 0.001*
RFOA	O1a	147.500	8.262	< 0.001*	39.500	8.042	< 0.001*
	O1b	135.000	8.334	< 0.001*	57.500	7.906	< 0.001*
	O2a	36.000	8.865	< 0.001*	10.000	8.222	< 0.001*
	O2b	23.500	8.938	< 0.001*	3.000	8.276	< 0.001*
SFOA	O1a	67.500	8.727	< 0.001*	13.500	8.239	< 0.001*
	O1b	67.000	8.730	< 0.001*	21.500	8.178	< 0.001*
	O2a	36.000	8.865	< 0.001*	10.000	8.222	< 0.001*
	O2b	23.500	8.938	< 0.001*	3.000	8.276	< 0.001*

Table 5 The shapes of the bordering of *foramina ovalia* and their visibility in connection to the species and age of tested individuals

			Species and age					
			P. leo ($n = 57$)			*P. tigris* ($n = 55$)		
			Adult ($n = 45$)	Juvenile ($n = 12$)	Total	Adult ($n = 49$)	Juvenile ($n = 6$)	Total
LFO	Semi-circular edge	Visible	6	0	6	37	4	41
	Straight edge	Visible	18	2	20	10	2	12
		Hidden	21	10	31	2	0	2
RFO	Semi-circular edge	Visible	10	1	11	37	4	41
	Straight edge	Visible	17	1	18	11	2	13
		Hidden	18	10	28	1	0	1

reliability and the inter-observer reliability in the case of RFOA measurements reached only moderate level. On the other hand, *foramina ovalia* do not have the potential to discriminate between sexes. In tigers, considerable variability was found in the orientation and shape of the *foramen ovale*, while in lions, this structure was relatively stable.

When using this feature in field practice, it is impossible, nevertheless, to measure the exact angle of the *foramen ovale*, especially since different observers may measure this angle slightly differently. However, it can be estimated whether the *foramina ovalia* point in a distinctly rostral (at an angle of less than 50°) or distinctly lateral (at an angle of more than 70°) direction, which our results show, are nearly diagnostic for identifying tiger and lion skulls, respectively.

In general, in the skull of an adult animal, if the *foramina ovalia* were visible from the ventral view, bordered by a semi-circular edge of the *os basisphenoidale* and pointing in a rostral direction, it was a tiger skull. No forward-facing *foramen ovale* was found on any lion skull. If the *foramina ovalia* were invisible, hidden behind the straight edge of the *os basisphenoidale* and pointing in a lateral direction, it was a lion skull. In our collection, this description was also fully consistent with juvenile lion skulls. The juvenile tiger skulls, on the other hand, had a *foramen ovale* structure markedly different from that of adult tiger skulls. The *foramina ovalia* of the juvenile tigers were directed laterally, but unlike the juvenile lion skulls, they were fully visible in all cases. However, given the small number of juveniles examined, it is impossible to determine whether this difference reflects higher variability found in *foramen ovale* formation in tigers or the ontogenetic development of this structure. Nevertheless, the age of animal must be considered when evaluating the skulls in the field.

Skulls in which the *foramina ovalia* could not be unambiguously assigned to the above types were found in both lions and tigers. In adult animals it included mainly skulls where the *foramina ovalia* were oblique (at an angle between 50° and 70°) or skulls where the *foramina ovalia* pointed laterally but were not hidden behind the straight edge of the *os basisphenoidale*. In these situations, it is necessary to evaluate other features that can distinguish tiger and lion skulls (Blanford 1888; Boule 1906; Pocock 1929; Merriam and Stock 1932; Haltenorth 1936, 1937; Hemmer 1966; Christiansen 2008; Christiansen and Harris 2009). This is, of course, advisable in any case to confirm the determination. A complex set of features distinguishable from photographs

that can be used to determine tiger and lion skulls in field practice was presented by Formanova et al. (2022).

The *foramen ovale* and its orientation on the cranial base of tiger and lion skulls can be successfully used to identify the skulls of these two species quickly. Rostrally orientated *foramen ovale* was detected only in tigers. In contrast, a laterally oriented *foramen ovale*, which is hidden behind the straight edge of the *os basisphenoidale* from the ventral view, was characteristic of lion skulls, including those of juveniles. Like the other characters described in the literature, *foramen ovale* cannot be used to distinguish the skulls of both species with absolute certainty. Combined with other characters, it can serve as one of the most determinative.

Supplementary Information The online version contains supplementary material available at https://doi.org/10.1007/s42991-023-00388-x.

Acknowledgements We are grateful to the staff of the Czech National Museum, Hodonin Zoo, Jihlava Zoo, Lesna Zoo, Liberec Zoo, Olomouc Zoo, Ostrava Zoo, Plzen Zoo, Safari Park Dvur Kralove, Bojnice Zoo, University of Veterinary Sciences Brno, Faculty of Science of Charles University in Prague, Czech Environmental Inspectorate, Customs Administration of the Czech Republic, and taxidermist Benjamin Hlivka for the access to their osteological collections.

Author contributions All authors contributed to the conception of the study. Data collection and study on skulls were performed by DF. MP and OH contributed to the data analysis. Statistical analysis was performed by AK. DF and AK drafted and finalized the manuscript. All authors participated in writing the manuscript. All authors read and approved the final version of the manuscript.

Funding Open access publishing supported by the National Technical Library in Prague. Open Access publishing was enabled by the CzechELib Transformative Agreement. This study was conducted as a part of project no. VJ01010026 Effective use of forensic evidence methods to combat wildlife crime financially supported by the Ministry of the Interior of the Czech Republic within the programme Strategic Support for the Development of Security Research 2019–2025 (IMPAKT 1).

Data availability The authors confirm that the data supporting the findings of this study are available within the article and its supplementary materials.

Declarations

Conflict of interest None known for all authors.

Open Access This article is licensed under a Creative Commons Attribution 4.0 International License, which permits use, sharing, adaptation, distribution and reproduction in any medium or format, as long as you give appropriate credit to the original author(s) and the source, provide a link to the Creative Commons licence, and indicate if changes were made. The images or other third party material in this article are included in the article's Creative Commons licence, unless indicated otherwise in a credit line to the material. If material is not included in the article's Creative Commons licence and your intended use is not permitted by statutory regulation or exceeds the permitted use, you will need to obtain permission directly from the copyright holder. To view a copy of this licence, visit http://creativecommons.org/licenses/by/4.0/.

References

Blanford WT (ed) (1888) The fauna of British India, including Ceylon and Burma. Mammalia. Taylor and Francis, London

Boule M (1906) Les grands chats des cavernes. Ann Paleontol 1:69–95

Christiansen P (2008) Distinguishing skulls of lions (*Panthera leo*) and tigers (*Panthera tigris*). Mamm Biol 73:451–456. https://doi.org/10.1016/j.mambio.2007.08.001

Christiansen P, Harris JM (2009) Craniomandibular morphology and phylogenetic affinities of *Panthera atrox*: implications for the evolution and paleobiology of the lion lineage. J Vertebr Paleontol 29:934–945. https://doi.org/10.1671/039.029.0314

Cooper DM, Yamaguchi N, Macdonald DW et al (2022) Phenotypic plasticity determines differences between the skulls of tigers from mainland Asia. R Soc Open Sci 9:220697. https://doi.org/10.1098/rsos.220697

EIA (2017) The lion's share: South Africa's trade exacerbates demand for tiger parts and derivatives. Environmental Investigation Agency (EIA). https://eia-international.org/wp-content/uploads/The-Lions-Share-FINAL.pdf

Feldesman MR (2002) Classification trees as an alternative to linear discriminant analysis. Am J Phys Anthropol 119:257–275. https://doi.org/10.1002/ajpa.10102

Formanova D, Pyszko M, Horak O, Rihova P, Novak Z (2022, October 30–November 4) Morphological differences between the skulls of tigers (*Panthera tigris*) and lions (*P. leo*) [conference presentation]. SWFS 2022, Ashland, Oregon, United States

Haltenorth T (1936) Die verwandtschaftliche Stellung der Großkatzen zueinander. I. Beschreibung der Schädelknochen. Z Säugetierkd 11:32–105

Haltenorth T (1937) Die verwandtschaftliche Stellung der Großkatzen zueinander VII. Z Säugetierkd 12:97–240

Hartstone-Rose A, Selvey H, Villari JR et al (2014) The three-dimensional morphological effects of captivity. PLoS ONE 9:e113437. https://doi.org/10.1371/journal.pone.0113437

Hemmer H (1966) Untersuchungen zur Stammesgeschichte der Pantherkatzen (Pantherinae). Teil I. Veröff Zool Staatssamml Münch 11:1–121

Koo TK, Li MY (2016) A guideline of selecting and reporting intraclass correlation coefficients for reliability research. J Chiropr Med 15:155–163. https://doi.org/10.1016/j.jcm.2016.02.012

Mazák JH (2010a) Geographical variation and phylogenetics of modern lions based on craniometric data. J Zool 281:194–209. https://doi.org/10.1111/j.1469-7998.2010.00694.x

Mazák JH (2010b) Craniometric variation in the tiger (*Panthera tigris*): implications for patterns of diversity, taxonomy and conservation. Mamm Biol 75:45–68. https://doi.org/10.1016/j.mambio.2008.06.003

Merriam JC, Stock C (1932) The Felidae of Rancho La Brea. Carnegie Institution of Washington, USA

Mills JA, Jackson P (1994) Killed for a cure: A review of the worldwide trade in tiger bone. TRAFFIC International, Cambridge, UK. https://www.traffic.org/site/assets/files/9563/killed-for-a-cure.pdf

Nittu G, Shameer TT, Nishanthini NK, Sanil R (2023) The tide of tiger poaching in India is rising! An investigation of the intertwined facts with a focus on conservation. GeoJournal 88:753–766. https://doi.org/10.1007/s10708-022-10633-4

Pocock RI (1929) Tigers. J Bombay Nat Hist Soc 33:505–541

Saragusty J, Shavit-Meyrav A, Yamaguchi N, Nadler R, Bdolah-Abram T, Gibeon L, Hildebrandt TB, Shamir MV (2014) Comparative skull analysis suggests species-specific captivity-related malformation in lions (*Panthera leo*). PLoS ONE 9:e94527. https://doi.org/10.1371/journal.pone.0094527

Schober P, Boer C, Schwarte LA (2018) Correlation coefficients: appropriate use and interpretation. Anesth Analg 126:1763–1768. https://doi.org/10.1213/ANE.0000000000002864

Shamir MH, Shilo Y, Fridman A, Chai O, Reifen R, Miara L (2008) Sub-occipital craniectomy in a lion (*Panthera leo*) with occipital bone malformation and hypovitaminosis A. J Zoo Wildl Med 39:455–459. https://doi.org/10.1638/2006-0064.1

Weir JP (2005) Quantifying test–retest reliability using the intraclass correlation coefficient and the SEM. J Strength Cond Res 19:231–240. https://doi.org/10.1519/15184.1

Williams VL, Loveridge AJ, Newton DJ, Macdonald DW (2015a) "Skullduggery": lions align and their mandibles rock! PLoS ONE 10:e0135144. https://doi.org/10.1371/journal.pone.0135144

Williams VL, Newton DJ, Loveridge AJ, MacDonald DW (2015b) Bones of contention: an assessment of the South African trade in African lion *Panthera leo* bones and other body parts. TRAFFIC, Cambridge, UK & WildCRU, Oxford, UK. https://www.traffic.org/site/assets/files/2474/bones_of_contention_report.pdf

Williams VL, Loveridge AJ, Newton DJ, Macdonald DW (2017) A roaring trade? The legal trade in *Panthera leo* bones from Africa to East-Southeast Asia. PLoS ONE 12:e0185996. https://doi.org/10.1371/journal.pone.0185996

Wilson DE, Reeder DAM (2005) Mammal species of the world: a taxonomic and geographic reference, 3rd edn. Johns Hopkins University Press, Baltimore

Wong R, Krishnasamy K (2022) Skin and bones: tiger trafficking analysis from January 2000–June 2022. TRAFFIC, Southeast Asia Regional Office, Petaling Jaya, Selangor, Malaysia. https://www.traffic.org/site/assets/files/19714/skin_and_bones_tiger_trafficking_analysis_from_january_2000_to_june_2022_r7.pdf

Yamaguchi N, Driscoll CA, Werdelin L et al (2013) Locating specimens of extinct tiger (*Panthera tigris*) subspecies: Javan tiger (*P. t. sondaica*), Balinese tiger (*P. t. balica*), and Caspian tiger (*P. t. virgata*), including previously unpublished specimens. Mammal Study 38:187–198. https://doi.org/10.3106/041.038.0307

Zuccarelli MD (2004) Comparative morphometric analysis of captive vs. wild African lion (*Panthera leo*) skulls. Bios 75:131–138. https://doi.org/10.1893/0005-3155(2004)075%3c0131:CMAOCV%3e2.0.CO;2

Publisher's Note Springer Nature remains neutral with regard to jurisdictional claims in published maps and institutional affiliations.